

# Ceramic-rubber hybrid materials – A way to sustain abrasive heavy impact applications

Marin Herr<sup>1,2</sup>, Markus Varga<sup>1</sup>, Jörg Mermagen<sup>2</sup>, Silvia Rodinger<sup>2</sup>, Wilfried Harwick<sup>2</sup>

<sup>1</sup>AC2T research GmbH, Viktor-Kaplan-Straße 2C, 2700, Wiener Neustadt, Austria

<sup>2</sup>Fraunhofer Institut für Kurzzeitdynamik, Ernst-Zermelo-Straße 4, 79104, Freiburg, Germany

## Abstract

Transport of raw materials in industrial applications usually involves highly abrasive processes and requires wear protection for a reliable, long operation period. At transfer points such as between conveyer belts additional impact loads can limit the lifetime. For such conditions rubber-ceramic hybrid materials can extend the lifetime multifold by combining the wear resistance of ceramics with the impact resistance of rubbers.

In this study the influence of design parameters for such hybrid solutions are numerically investigated. The material models used are based on model test with various strain rates to resemble the real loading conditions in the compound.

The investigations show the occurring stresses in the ceramic are influenced intensely by varying the area and thickness of the ceramic plates. Improvements on the design of the rubber backing and the rubber type can also significantly reduce the occurring stresses. These relations were mathematically retained and practical recommendations for the designs of the ceramic-rubber plates were given.

## 1 Introduction

Technical ceramics are known for high stiffness and hardness as well as very good temperature and corrosion resistance [1]. Alumina is the most widely used ceramic in industrial applications. Due to its very good wear resistance, it is often used in abrasive or erosive environments as wear protection [2,3]. The brittle behavior of these materials, however, can limit their application for environments with additional impact loads [4].

Improvements for the impact resistance of alumina ceramic could be achieved with laminated ceramics and functionally graded composites [5,6], two step sintering [7] or fiber reinforcement [8-11]. These improved ceramics often involve complex manufacturing processes and are thereby much more cost intensive and cannot compete with other wear protection solutions from an economical point of view [12-14].

Elastomers on the other hand are excellent for impact loads due to their viscoelastic behavior and shock absorbing abilities, but they lack resistance against abrasive wear. The combination of elastomers with ceramic materials can result in an economic wear protection for combined impact-abrasive loaded environments. The idea to combine the two materials to an impact resistant wear protection was already patented for conveyers and chutes in 1971 to ensure the shock resistance by preventing cracking of the ceramics at impact loads [15].

This work focuses on developing a systematic approach to optimize design parameters of a hybrid wear protection for a specific condition given in the practical application. Therefore, the mechanical characterization and modelling of ceramic and rubber materials with high availability was performed at different strain rates to use the properties in numerical simulations and to systematically evaluate the influence of different configurations, since each material can have significant influence on the overall physical behavior [16].

The time-explicit solver LS-DYNA was used to perform impact simulations. Such impact simulations are widely applied especially in the field of ballistic investigations on layered armor composites. In these investigations the focus is the absorption of the kinetic energy by the ceramic layers and transmission of the energy to the polymer backings [17–22]. For this project the goal is the non-destructive energy absorption and so the focus lays on the maximum stresses occurring in the ceramic tiles, since this is the main cause for fraction and failure of the whole compound.

Design parameters such as the size of the ceramic tile (area and thickness), the rubber thickness and rubber type were varied to determine the relations between the maximum stresses occurring.

## 2 Experimental material characterization

The hybrid wear protection is applied in severe wear environments. While the ceramic is carrying most of the wear loading the rubber between the ceramic plates will also be exposed some abrasive load and needs a reasonable wear resistance. For this application a black NR-SBR (natural rubber – styrene-butadiene rubber) with a Shore A hardness of  $65 \pm 3$  was used [23]. Rubber thicknesses from 6 ... 20 mm were investigated. To determine the influence of the rubber hardness a second softer rubber (of red color) was included in this work ( $45 \pm 4$  Shore A) [24].

Typically, the ceramic-rubber hybrid plates are tiled with cost-efficient alumina wear ceramic. For this study 92% alumina [25] was used as it showed good results in a pre-study in which the wear resistance of different ceramic materials were tested. Ceramic tiles of  $100 \times 100 \times 13$  mm were used for investigation. For the model tests these tiles were cut and plane grounded by to the dimensions needed in the physical experiments. For the impact tests the ceramic plates were glued to rubber tiles with same dimension in horizontal axes.

For a proper material modelling the ceramic and the two rubber materials were undergoing numerous mechanical tests at different strain rates of up to  $100 \text{ s}^{-1}$ . The tests and main test parameters are summarized in Table 1.

For characterization of the elastic properties of the ceramic material compression tests on  $48 \times 10 \times 10$  mm specimen were performed. The force signal from the load cell was used to derive the stress in the specimen and the strain was measured optically by monitoring a speckle pattern on the specimen surface with a high-speed camera. Over the lateral strain the Poisson's ratio of the material could also be determined [cf. 26]. To characterize the fracture behavior, the ceramic specimens were tested on a three point bending tests with a span length of 90 mm. The  $18 \times 13 \times 100$  mm samples were then loaded at cross-head speeds of 0.004 and 4 mm/s, which results in strain rates of  $3.66 \cdot 10^{-5}$  and  $3.66 \cdot 10^{-2} \text{ s}^{-1}$  at the outer fibers of the specimens. The deformation of the specimens was also monitored optically to compare the elastic response of this test with the compression test [cf. 27].

For characterization of the rubber materials tensile tests at strain rates of 0.01, 1, and  $100 \text{ s}^{-1}$  were performed to determine the visco-hyperplastic material behavior and the compression modulus [cf. 28]. Since the rubber material is deformed under compression load within the hybrid plate, additional uniaxial compression test on  $20 \times 20 \times 20$  mm cubic specimen at strain rates from 0.01 ...  $100 \text{ s}^{-1}$  were carried out to refine the model for this type of deformation [cf. 29].

The here investigated conditions involve the transport of HBIs (hot briquetted iron) for steel production with a maximal impact energy on 60 J (3 m drop height with a 2 kg mass). The material properties of the HBI impactor do have a significant effect on the occurring stresses. The quality and consequently properties of the steel at that state varies a lot. To investigate only critical conditions the material properties are assumed to be similar to a typical structural steel and have a spherical shape.

Table 1: Main parameters of the mechanical material model tests.

Tested material	test	Specimen size in mm	Strain rate in $\text{s}^{-1}$	Determined parameter
Ceramic	Uniaxial compression	$10 \times 10 \times 48$	$1 \cdot 10^{-4}$ , $1 \cdot 10^{-2}$	Young's modulus, Poisson's ratio
	3-point bending test	$18 \times 13 \times 100$	$3.66 \cdot 10^{-5}$ , $3.66 \cdot 10^{-2}$	Failure stress
Rubber (2 types)	Tensile test	$12 \times 6 \times 30$	0.01, 1, 100	Visco-hyperplastic response, Poisson's ratio
	Uniaxial compression	$20 \times 20 \times 20$	0.01, 0.1, 1, 10, 50, 100	Model refinement for compressive load

## 3 Numerical set-up

The base model of the ceramic-rubber hybrid plate consists of a ceramic tile ( $100 \times 100 \times 13$  mm) (Fig. 1 in red), a rubber backing (5 mm in thickness, Fig. 1 in blue) and a spherical impactor ( $\varnothing 20$  mm) (Fig. 1 in green). To describe the linear elastic material behavior of the ceramic the element nodes of the bottom surface of the rubber are fixed, while the rest of the elements can deform freely.

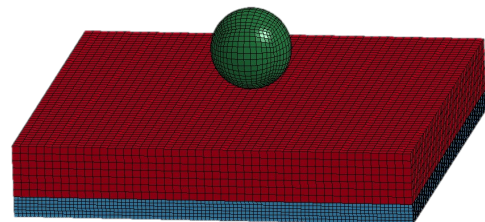


Figure 1: Numerical set-up of base model impact simulation in LS-Dyna.

The initial velocity of the impactor is set to 7.75 m/s and density was scaled up to reach a mass of 2 kg (60 J impact energy). The mechanical property of the ceramic is described by a linear elastic material model (\*MAT\_001 in LS-Dyna), for the rubber the hyperplastic material model (\*MAT\_077\_H) was chosen. The mechanical response of the impactor is described by a bilinear model (\*MAT\_024).

The element size of the ceramic plate is chosen to be seven elements in height. Due to the linear element formulation the maximum element stress due to bending of the plate is underestimated by 16.67%. This stress signal is corrected in the data post-processing. The rubber backing is divided into six element layers. The number of elements over the thickness is hold constant for variations in the geometries. The base model consists of 90 000 elements.

To investigate the influence of different design parameters the geometry, surface area, ceramic thickness and rubber thickness and type are varied from the base model to see the direct influence for these specific configurations.

## 4 Results

### 4.1 Mechanical properties of the materials

The mechanical testing was performed to characterize the material behavior and determine exact parameters for the material models. The Young's modulus for the compression test of the ceramic was determined to be  $E = 278 \pm 8$  GPa with a Poisson's ratio of 0.22. For the bending test a Young's modulus of  $276 \pm 16$  GPa was found, which indicates a isotropic material behavior with no visible strain rate effects. Based on these results the elastic material parameters for the ceramic were set to  $E = 278$  GPa with a Poisson's ratio of 0.22.

The failure stress of the ceramic material at bending tests was in the range between 175—221 MPa for slow loading and 223—251 MPa for higher loading speeds. Applying the Weibull analysis [30] for the failure probability and determining the subcritical crack growth parameters [31] gave a failure stress of 180 MPa at a failure probability of 1% for a  $100 \times 100 \times 13$  mm ceramic plate size for high-speed loading. The material characterization of the two rubber materials showed, as expected from the hardness, a stiffer material behavior of the black rubber for the uniaxial tension and compression tests. Both materials display a clear increase of the stresses with increased strain rates, which indicates the importance of including the viscose material response. The determined material parameters can be found in Table 2.

Table 2: Material parameters as used in the hyperelastic model of the rubbers

<i>rubber</i>	<i>Elastic material parameters</i>	<i>Spring-slider parameter</i>	<i>Viscose material parameter</i>	<i>Density</i>
<i>black</i>	$C10 = 0.67$ MPa $C01 = 0$ MPa $PR = 0.43$	$G = 4.24$ MPa $S = 0.2$ MPa	$G1 = 0.2$ MPa, $BETA1 = 3.0$ s <sup>-1</sup> $G2 = 0.4$ MPa, $BETA2 = 100$ s <sup>-1</sup> $G3 = 9.5$ MPa, $BETA3 = 3000$ s <sup>-1</sup>	1.15 g/cm <sup>3</sup>
<i>red</i>	$C10 = 0.25$ MPa $C01 = 0.0098$ MPa $PR = 0.49$	$G = 0$ MPa $S = 0$ MPa	$G1 = 0.025$ MPa, $BETA1 = 3.0$ s <sup>-1</sup> $G2 = 0.14$ MPa, $BETA2 = 300$ s <sup>-1</sup> $G3 = 1.5$ MPa, $BETA3 = 10000$ s <sup>-1</sup>	1.06 g/cm <sup>3</sup>

### 4.2 Simulation results

At first a central impact on the base model was performed to analyze the stress response of the hybrid system. The typical stress response consists of two peaks (see Fig. 2). The first peak at ~0.25 ms results from inertia effects of the ceramic tile. This spike can not be influenced by the rubber backing but by the ceramic size. The second peak arises due to the bending stresses and is significantly influenced by the rubber backup. A poor choice of the design parameters could result in a high stress peaks in one of the parts that results in failure of the tile. Ideally both spikes have the same height and are just below the maximum tolerated stresses.

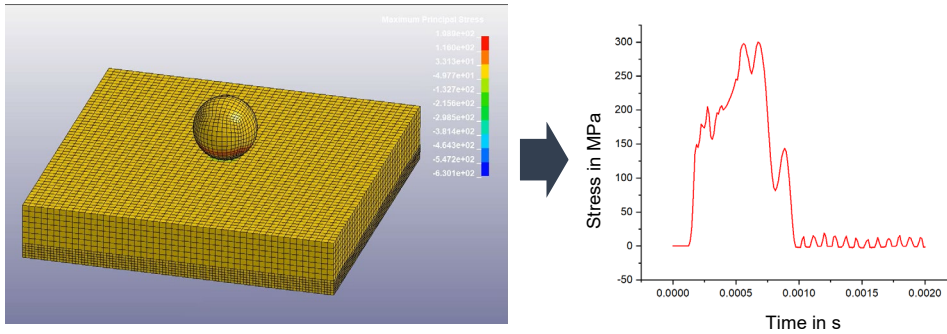


Figure 2: Stress response of impact on base model.

In a first design parameter variation the influence of different surface geometries was investigated. The different shapes can be seen in Fig. 3. The surface area of each of the geometries has the same size. The rectangular shape (aspect ratio 1:2) showed an increase of the stress of ca. 40%, while the circular and hexahedral shape do not show any significant increase of stress. As a conclusion the quadratic shape is recommended, as the other shapes are more complex to produce and less economical.

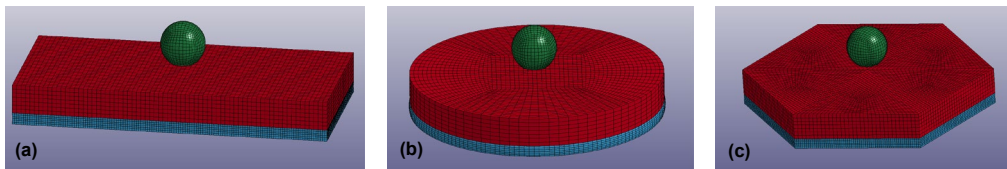


Figure 3: Variation of the surface geometry to a (a) rectangle, (b) circle, (c) hexagon.

In the second parameter study the surface size of the ceramic tiles was varied on the quadratic shape. The surface sizes of 10 000 mm<sup>2</sup>, 5 000 mm<sup>2</sup> and 2 500 mm<sup>2</sup> were studied. The simulation shows a significant decrease in the stress response of the ceramic tile. The proportional relationship between surface area and maximum stress could be mathematically described with:

$$\sigma_{max} \propto \sqrt{A} \quad \text{Eq. 1}$$

In a third study the thickness of the ceramic tile was changed from 6.5 mm up to 26 mm. By increasing the thickness of the ceramic plate the stresses decreased significantly. The following mathematically approximation could be found:

$$\sigma_{max} \propto \frac{1}{t_c^2} \quad \text{Eq. 2}$$

In the last study the influence of increasing the rubber backing was investigated. For the following set-up rubber thicknesses of 2.5 mm, 5 mm, 10 mm and 20 mm were numerically tested. The stresses in the ceramic decreased with increasing rubber thicknesses. The relationship between stress and thickness can be mathematically described as

$$\sigma_{max,black} \propto t_R^{-0.16} \quad \text{Eq. 3}$$

for the black (harder) rubber and

$$\sigma_{max,red} \propto t_R^{-0.24} \quad \text{Eq. 4}$$

for the red (softer) rubber. A slight curvature at the data points indicates a minimum stress limit for very thick rubber backings and a maximum stress limit for very thin rubber backings [4].

## 5 Discussion

The numerical parameter study showed the influence on the occurring stresses in the ceramic and thereby gives guidance to improve the impact resistance of the hybrid solution. If the installation space is limited in height (or weight) the only option to improve the impact resistance is by decreasing the surface area of the of the ceramic tiles. This however is increasing the total edge length of the ceramic which causes more wear at the high loaded edges.

By increasing the thickness of the ceramic, the impact resistance can also be improved significantly. However, it also increases the total costs of the wear protection, as the alumina ceramic causes most of the costs in the ceramic-rubber wear protection.

Increasing the rubber backing can be a cost-efficient solution to improve the impact resistance of the compound. The improvement is however highly dependent on the current set-up. An already sufficient rubber backing will not improve the impact resistance, if additional rubber backing is added, especially if the stress spike caused by the inertia of the ceramic tile causes the highest stress during impact. An insufficient rubber backing can be improved significantly with additional rubber thickness.

Changing the surface geometry of the ceramic tile showed no improvement and is not recommended due to higher production costs of non-quadratic solutions.

The hardness of the rubber backing also shows a considerable influence. Depending on the rubber type the optimal design parameters of the backing can differ. A proper material characterization of the viscoelastic material response is recommended.

## 6 Summary

In this study the stress response in a ceramic tile of a ceramic-rubber hybrid wear protection due to impact load is investigated numerically. This is used to predict the necessary setup to prevent fracture and early failure of the wear protection in practical applications.

The investigated materials from industrial use (92% alumina ceramic and two rubbers with different Shore hardness) were characterized by mechanical tests at strain rates up to 100 s<sup>-1</sup>. The so gained parameters were used to setup a time-explicit simulation in LS-Dyna and make parameter studies of different geometrical parameters to identify ideal parameter sets for optimal material input vs. lifetime of the hybrid solutions.

The typical stress response in the ceramic consists of a first stress spike due to inertia effects of the tile and a second stress spike due to bending of the tile caused by the rubber backing. The first stress spike can not be influenced by the rubber backing but by the ceramic size, while the second spike is mainly characterized by the behavior of the rubber.

When varying the ceramic shape, hexagonal or circular tiles do not improve the stress response and so the quadratic shape should be favored due to simpler production. Decreasing the surface area of the ceramic tile decreases the stresses in the ceramic and so improves the impact resistance. The proportional relationship  $\sigma_{max} \propto \sqrt{A}$  was identified. Increasing the thickness of the ceramic tile also decreases the maximal stress ( $\sigma_{max} \propto \frac{1}{t_c^2}$ ).

Increasing the rubber backing thickness can improve the impact resistance the here found relationships are  $\sigma_{max,red} \propto t_R^{-0.24}$  and  $\sigma_{max,red} \propto t_R^{-0.16}$  these values however are dependent of the current set-up. However, the difference in the exponents shows that the rubber properties have a significant influence on the stress response.

## Acknowledgments

This work was funded by the “Austrian COMET-Program” (project InTribology, no. 872176) via the Austrian Research Promotion Agency (FFG) and the Province of Niederösterreich, Vorarlberg and Wien and was carried out within the “Excellence Centre of Tribology” (AC2T research GmbH). Special thanks go to Mr. Wilfried Harwick at Fraunhofer EMI for fruitful discussions and to Voestalpine GmbH and Wanggo Gummitechnik GmbH for the active research cooperation.

## 7 Literature

- [1] Chunxin Liu, Alternative Binder Phases for WC Cemented Carbides, Master Thesis, KTH, Stockholm, 2014.
- [2] M. Varga, K. Adam, M. Tumma, K.O. Alessio, Abrasive wear of ceramic wear protection at ambient and high temperatures, J. Phys. Conf. 843 (1) (2017).
- [3] M. Varga, M. Antonov, M. Tumma, K. Adam, K.O. Alessio, Solid particle erosion of refractories: a critical discussion of two test standards, Wear 426 (2019) 552–561.
- [4] M. Varga, M. Herr, L. Widder, L. A. de Campos, J. Mermagen, Ceramic-rubber hybrid materials—A knowledge-based design concept. Wear (2021): 203735.
- [5] L. Li, L. Cheng, S. Fan, X. Gao, Y. Xie, L. Zhang, A novel fabrication approach for impact resistance laminated ceramics, Mater. Des. 79 (2015) 26–31.
- [6] C.Y. Huang, Y.L. Chen, Design and impact resistant analysis of functionally graded Al<sub>2</sub>O<sub>3</sub>–ZrO<sub>2</sub> ceramic composite, Mater. Des. 91 (2016) 294–305.

- [7] N.J. Lóh, L. Simão, J. Jiusti, S. Arcaro, F. Raupp-Pereira, A. De Noni Jr., O.R.K. Montedo, Densified alumina obtained by two-step sintering: impact of the microstructure on mechanical properties, *Ceram. Int.* 46 (8B) (2020) 12740–12743.
- [8] D. Gregori, R. Scazzosi, S.G. Nunes, S.C. Amico, M. Giglio, A. Manes, Analytical and numerical modelling of high-velocity impact on multilayer alumina/aramid fiber composite ballistic shields: improvement in modelling approaches, *Compos. B Eng.* 187 (2020), 107830.
- [9] S.A.B. Lins, M.C.G. Rocha, J.R.M. d’Almeida, Mechanical and thermal properties of high-density polyethylene/alumina/glass fiber hybrid composites, *J. Thermoplast. Compos. Mater.* 32 (11) (2019) 1566–1581.
- [10] A. Licciulli, A. Chiechi, M. Fersini, K.P. Sanosh, A. Balakrishnan, Influence of zirconia interfacial coating on alumina fiber-reinforced alumina matrix composites, *Int. J. Appl. Ceram. Technol.* 10 (2) (2013) 251–256.
- [11] W.K. Jung, H.S. Lee, J.W. Jung, S.H. Ahn, W.I. Lee, H.J. Kim, J.W. Kwon, [Retraction] penetration mechanisms of ceramic composite armor made of alumina/GFRP, *Int. J. Precis. Eng. Manuf.* 8 (4) (2007) 38–44.
- [12] S.D. Viljoen, Reduced maintenance costs resulting from the use of wear resistant materials, *J. S. Afr. Inst. Mining Metall.* 110 (7) (2010) 351–359.
- [13] H. Rojacz, I.A. Neacso, L. Widder, M. Varga, J. Heiß, Thermal effects on wear and material degradation of slag pots operating in steel production, *Wear* 350 (2016) 35–45.
- [14] H. Rojacz, M. Premauer, M. Varga, Alloying and strain hardening effects in abrasive contacts on iron based alloys, *Wear* 410 (2018) 173–180.
- [15] Beninga, D. H. (1971). U.S. Patent No. 3,607,606. Washington, DC: U.S. Patent and Trademark Office.
- [16] S. Salaeh, N. Muensit, P. Bomlai, C. Nakason, Ceramic/natural rubber composites: influence types of rubber and ceramic materials on curing, mechanical, morphological, and dielectric properties, *J. Mater. Sci.* 46 (6) (2011) 1723–1731.
- [17] H. Mahfuz, Y. Zhu, A. Haque, A. Abutalib, U. Vaidya, S. Jeelani, B. Fink, Investigation of high-velocity impact on integral armor using finite element method, *Int. J. Impact Eng.* 24 (2) (2000) 203–217.
- [18] S. Mahdi, J.W. Gillespie, Finite element analysis of tile-reinforced composite structural armor subjected to bending loads, *Compos. B Eng.* 35 (1) (2004) 57–71.
- [19] A. Gositanon, M. Chaiyarit, S. Phabjanda, Ballistic simulation and verification of ceramic/rubber composite armour, in: 2018 6th International Conference on Mechanical, Automotive and Materials Engineering (CMAME), IEEE, 2018, pp. 18–22.
- [20] A. Tasdemirci, G. Tunusoglu, M. Güden, The effect of the interlayer on the ballistic performance of ceramic/composite armors: experimental and numerical study, *Int. J. Impact Eng.* 44 (2012) 1–9.
- [21] N.K. Naik, S. Kumar, D. Ratnaveer, M. Joshi, K. Akella, An energy-based model for ballistic impact analysis of ceramic-composite armors, *Int. J. Damage Mech.* 22 (2) (2013) 145–187.
- [22] Z. Wang, P. Li, A model incorporating damage evolution to predict the penetration behavior of a ceramic target subjected to the long projectile impact, *Int. J. Impact Eng.* 135 (2020) 103393.
- [23] Semperit Black Star, Product Datasheet in Product Catalogue, 18.11.2008.
- [24] Semperit Red Star, Product Datasheet in Product Catalogue, 18.11.2008.
- [25] Kalenborn KALOCER HD, Material Data Sheet, 5.3.2020.
- [26] ISO 20504, Fine Ceramics (Advanced Ceramics, Advanced Technical Ceramics) — Test Method for Compressive Behaviour of Continuous Fibre-Reinforced Composites at Room Temperature, 2006.
- [27] DIN EN 843-1, Hochleistungskeramik - Mechanische Eigenschaften monolithischer Keramik bei Raumtemperatur - Teil 1: Bestimmung der Biegefestigkeit, 2008-08.
- [28] DIN EN ISO 527, Kunststoffe - Bestimmung der Zugeigenschaften, 2019.
- [29] ISO 7743:2017. Rubber, Vulcanized or Thermoplastic — Determination of Compression Stress-Strain Properties.
- [30] D. Mutz, T. Fett, *Mechanisches Verhalten Keramischer Werkstoffe*, Springer Verlag, Berlin Heidelberg, 1989.
- [31] DIN EN 843-3, Hochleistungskeramik – Mechanische Eigenschaften monolithischer Keramik bei Raumtemperatur – Teil 3: Bestimmung der Parameter des unterkritischen Risswachstums aus Biegefestigkeitsprüfungen mit konstanter Spannungsrate, 2005-08.